Applied Radiation and Isotopes 195 (2023) 110737

Contents lists available at ScienceDirect

Applied Radiation and Isotopes

journal homepage: www.elsevier.com/locate/apradiso

Optimized production of ^{67}Cu based on cross section measurements of ^{67}Cu and ^{64}Cu using an 18 MeV medical cyclotron

Gaia Dellepiane [a,*], Pierluigi Casolaro [a], Alexander Gottstein [a], Isidre Mateu [a], Paola Scampoli [a,b], Saverio Braccini [a]

[a] Albert Einstein Center for Fundamental Physics (AEC), Laboratory for High Energy Physics (LHEP), University of Bern, Sidlerstrasse 5, CH-3012 Bern, Switzerland

[b] Department of Physics "Ettore Pancini", University of Napoli Federico II, Complesso Universitario di Monte S. Angelo, 80126 Napoli, Italy

ARTICLE INFO

Keywords:
Copper-67
Theranostics
Cross sections
Proton irradiation
Medical cyclotron
Solid targets
Targeted radionuclide therapy

ABSTRACT

RadioNuclide Therapy (RNT) in nuclear medicine is a cancer treatment based on the administration of radioactive substances that specifically target cancer cells in the patient. These radiopharmaceuticals consist of tumor-targeting vectors labeled with β^-, α, or Auger electron-emitting radionuclides. In this framework, ^{67}Cu is receiving increasing interest as it provides β^--particles accompanied by low-energy γ radiation. The latter allows to perform Single Photon Emission Tomography (SPECT) imaging for detecting the radiotracer distribution for an optimized treatment plan and follow-up. Furthermore, ^{67}Cu could be used as therapeutic partner of the β^+-emitters ^{61}Cu and ^{64}Cu, both currently under study for Positron Emission Tomography (PET) imaging, paving the way to the concept of theranostics. The major barrier to a wider use of ^{67}Cu-based radiopharmaceutical is its lack of availability in quantities and qualities suitable for clinical applications. A possible but challenging solution is the proton irradiation of enriched ^{70}Zn targets, using medical cyclotrons equipped with a solid target station. This route was investigated at the Bern medical cyclotron, where an 18 MeV cyclotron is in operation together with a solid target station and a 6-m-long beam transfer line. The cross section of the involved nuclear reactions were accurately measured to optimize the production yield and the radionuclidic purity. Several production tests were performed to confirm the obtained results.

1. Introduction

With an average content of (1.4÷2.1) mg/kg, copper is the third most abundant metal after iron and zinc (IAEA, 2016) in the human body and it is necessary for the proper functioning of organs and metabolic processes (Chen et al., 2020). Along with the growth of theranostics and personalized medicine, copper radioisotopes are attracting increasing interest as they are characterized by a wide range of half-lives and several decay modes. Among them, ^{60}Cu [$t_{1/2}$ = 23.7 min], ^{61}Cu [$t_{1/2}$ = 3.339 h] and ^{62}Cu [$t_{1/2}$ = 9.67 min] are pure β^+-emitters and can be used for PET imaging; ^{64}Cu [$t_{1/2}$ = 12.7006 h] undergoes three different decays, namely electron capture (44%), β^--decay (38.5%) and β^+-decay (17.5%), and it finds application in both the diagnostic and the therapeutic fields. ^{67}Cu [$t_{1/2}$ = 61.83 h] is the longest-living copper radioisotope, whose emission comprises low-energy β^--particles [$E^{max}_{\beta-}$ = 377 keV (57%); 468 keV (22%); 562 keV (20%)] and γ-rays [E_γ = 185 keV (49%); 92 keV (23%)]. These characteristics make it suitable for RNT and it allows for SPECT imaging during treatment.

Compared to the clinically-established ^{177}Lu [$t_{1/2}$ = 6.64 d, $E^{max}_{\beta-}$ = 497 keV (79%); 176 keV (12%), E_γ = 208 keV (10%); 113 keV (6%)], ^{67}Cu has a similar β^- range, but its shorter half-life allows it to be used for labeling molecules with a faster washout from tumor tissues (Champion et al., 2016). Furthermore, it offers the advantage of having diagnostic radioisotope partners, forming the ^{64}Cu/^{67}Cu and ^{61}Cu/^{67}Cu true theranostic pairs. Copper radioisotopes potentially allow the most accurate picture of the radiopharmaceutical distribution prior to radionuclide therapy via both SPECT and PET.

Despite its potential, the limited availability of ^{67}Cu in quantities and qualities suitable for medical applications makes it rarely used in clinical settings. Only recently ^{67}Cu has become available in the U.S. through the Department of Energy Isotope Program (DOE-IP) (Merrick

* Corresponding author.
E-mail address: gaia.dellepiane@lhep.unibe.ch (G. Dellepiane).

https://doi.org/10.1016/j.apradiso.2023.110737
Received 8 December 2022; Received in revised form 20 January 2023; Accepted 19 February 2023
Available online 21 February 2023

Table 1
^{67}Cu production routes.

Impinging particle	Target	Route	Energy range [MeV]
p	^{70}Zn	(p,α)	25–10 (Levkowskij, 1991; Kastleiner et al., 1999)
p	^{68}Zn	(p,2p)	70–35 (Morrison and Caretto, 1962, 1964; McGee et al., 1970; Levkowskij, 1991; Schwarzbach et al., 2001; Stoll et al., 2002; Szelecsényi et al., 2009; Pupillo et al., 2018)
p	^{70}Zn + ^{68}Zn	(p,x) + (p,2p)	70–55 + 55–35 (Pupillo et al., 2020; Mou et al., 2021)
d	^{70}Zn	(d,x)	26–16 (Kozempel et al., 2012; Nigron et al., 2021)
α	^{64}Ni	(α,p)	30–10 (Tanaka, 1960; Levkowskij, 1991; Skakun and Qaim, 2004; Takács et al., 2020)
γ	^{68}Zn	(γ,x)	60–30 (Starovoitova et al., 2011; Aliev et al., 2019; Hovhannisyan et al., 2021)
n	^{67}Zn	(n,p)	> 1 (Kielan and Marcinkowski, 1995; Nesaraja et al., 1999; Shimizu et al., 2004; Furuta et al., 2008; Bhike et al., 2009; Uddin et al., 2014; Johnsen et al., 2015)

Table 2
Physical properties and main γ emissions of the radionuclides of interest (IAEA, 2022). The values in parentheses are the uncertainties referred to the last digits of the value. I is the intensity of the γ line.

Radionuclide	$t_{1/2}$	Decay mode: [%]	E_γ [keV]	I_γ [%]
^{64}Cu	12.7006(20) h	ec + β^+: 61.5 β^-: 38.5	1345.77(6) –	0.472(4) –
^{67}Cu	61.83(12) h	β^-: 100	93.311(5) 184.577(10)	16.1(2) 48.7(3)
^{67}Ga	3.2617(5) d	ec: 100	93.310(5) 184.576(10)	38.81(3) 21.41(1)

Table 3
Isotopic abundance of the enriched ^{70}ZnO powder supplied by CortecNet and the enriched ^{68}Zn foil supplied by ISOFLEX.

	^{64}Zn	^{66}Zn	^{67}Zn	^{68}Zn	^{70}Zn
^{70}ZnO-enr. [%]	0.02	0.01	0.02	1.20	98.75
^{68}Zn-enr. [%]	0.99	0.81	0.38	97.80	0.02

et al., 2021). The investigation of ^{67}Cu supply worldwide is therefore a crucial point and in particular its production has been studied through various nuclear reactions (Table 1). In the framework of a research program aimed at the production of copper radioisotopes for theranostics (Dellepiane et al., 2022e,c) at the Bern medical cyclotron laboratory, ^{67}Cu production via proton irradiation of enriched ^{70}ZnO solid targets was considered.

The only copper impurity using this route is ^{64}Cu, produced in traces for energies above 14 MeV via the secondary reaction ^{68}Zn(p,αn)^{64}Cu. Since ^{68}Zn is present as impurity in the enriched ^{70}ZnO, the cross section of this reaction was measured by irradiating enriched ^{68}Zn targets. The results were then normalized to the isotopic abundance of ^{68}Zn in the enriched ^{70}Zn material to study the ^{64}Cu production yield.

^{67}Ga is also produced during the irradiation through the ^{68}Zn(p,2n)^{67}Ga nuclear reaction. Although it does not affect the radionuclidic purity of ^{67}Cu, it presents the same γ-lines (Table 2) and its contribution must be disentangle for cross section calculations.

On the basis of the obtained results, a study of the production yield and radionuclidic purity of ^{67}Cu was performed to optimize the irradiation parameters. Several production tests were carried out by irradiating enriched ^{70}ZnO solid targets.

2. Materials and methods

2.1. The Bern medical cyclotron laboratory

The Bern University Hospital (Inselspital) (Braccini, 2013) hosts an IBA Cyclone 18/18 HC (High Current) cyclotron, accelerating H^- ions to a nominal energy of 18 MeV with a current range from a few pA to 150 μA (Auger et al., 2015). The cyclotron features six ^{18}O-enriched water targets for the industrial production of ^{18}F, an IBA Nirta Solid Target Station (STS) and a 6-m-long Beam Transfer Line (BTL) that brings the beam to a bunker, with independent access, dedicated to research activities. This solution is uncommon for a hospital-based facility and allows the spin-off company Swan Isotopen AG to synthesize ^{18}F-labeled tracers for PET imaging overnight and the Laboratory for High Energy Physics (LHEP) of the University of Bern to perform multidisciplinary research during the day (Braccini and Scampoli, 2016). The BTL is equipped with beam focusing and diagnostic systems, including a non-destructive two-dimensional beam profiler based on scintillating doped silica fibers passing through the beam. The detector, named UniBEaM, was developed by our group and commercialized by the company D-Pace (Auger et al., 2016; Potkins et al., 2017). The BTL is characterized by an extracted beam energy of (18.3 ± 0.3) MeV (Nesteruk et al., 2018; Häffner et al., 2019) and it was used for the cross section measurements presented in this paper.

The ^{67}Cu production tests were performed using the STS. It is connected to the cyclotron through an apparatus based on a compact focusing and steering magnet system, named Mini-PET Beamline (MBL) (Dehnel et al., 2013), followed by a UniBEaM detector. This system was conceived to optimize the irradiation procedure, allowing to control the size and position of the beam and to keep it on the target by correcting its possible deviations using the MBL (Häffner et al., 2021). The STS was customized with automatic target loading and delivery systems to minimize the dose to personnel (Dellepiane et al., 2022b). In particular, the irradiated target can be sent either to a hot-cell in the nearby GMP radio-pharmacy or to a receiving station located in the BTL bunker. The latter option is used when the target is transported to external laboratories for chemical processing or transferred to the physics laboratory of the facility for γ spectrometry. A N-type high purity germanium (HPGe) detector (Canberra2019) is used for this purpose. The detector is coupled to a preamplifier and to a Lynx® digital signal analyzer. The spectrum of the source is acquired with the Genie2K software (Mirion Technologies, 2022) in the case of a single measurement and with the Excel2Genie (Forgács et al., 2014) Microsoft Excel application for repeated measurements. The analysis is carried out with the InterSpec software (Sandia National Laboratories, 2022), developed by the Sandia National Laboratories. The efficiency calibration was performed in accordance with the international standard (International Standard, 2021) by means of a multi-peak γ source containing ^{57}Co, ^{60}Co, ^{85}Sr, ^{88}Y, ^{109}Cd, ^{133}Sn, ^{137}Cs and ^{241}Am, and resulted in efficiency uncertainties below 3%.

The production of ^{67}Cu was studied by irradiating a 98.75% enriched ^{70}ZnO powder, purchased by CortecNet (Cortecnet, 2022). To measure the ^{68}Zn(p,αn)^{64}Cu nuclear reaction cross section, a 97.80% enriched ^{68}Zn foil by Isoflex (Isoflex, 2022) was used. The isotopic compositions of the two materials are reported in Table 3.

2.2. Cross section measurements

Targets for cross section measurements were prepared with the sedimentation method. Aluminum disks (22.8 mm in diameter, 2 mm thick) with a 4.2-mm diameter and 0.8-mm deep pocket in their center were used as backing (Fig. 1-a). A few milligrams of ZnO powder was suspended in distilled water and deposited in the pocket (Fig. 1-b). Once the water had completely evaporated by means of a heating plate, the deposited mass was measured with an analytical balance

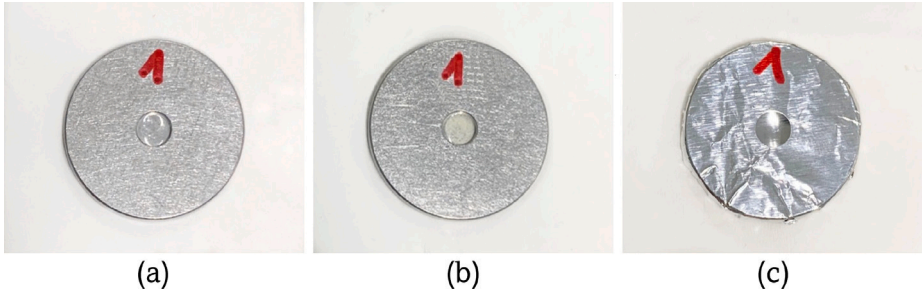

Fig. 1. Target preparation procedure used for cross section measurements: (a) empty aluminum disk; (b) aluminum disk filled with enriched ^{70}ZnO powder; (c) aluminum disk covered with a 13-μm-thick aluminum foil.

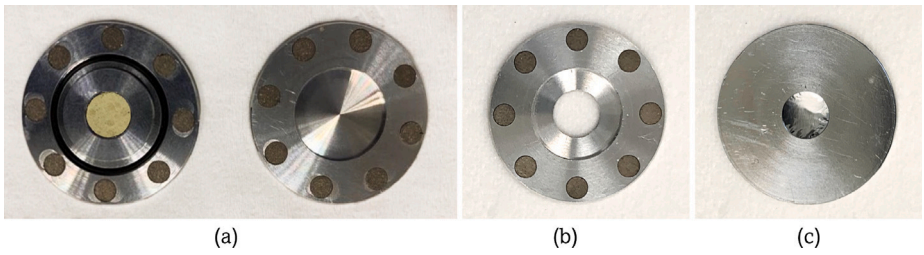

Fig. 2. (a) The cup containing the 6-mm pellet (left) and the lid (right) of the coin target; (b) lid with a 7-mm-diameter hole; (c) 13-μm-thick aluminum foil inserted inside the coin to prevent the pellet leakage during the irradiation.

(Mettler Toledo AX26 DeltaRange). The measurement uncertainty was within 5%. Finally, the target was sealed with a 13-μm-thick aluminum foil (Fig. 1-c) to guarantee that the material is kept within the pocket throughout the irradiation and measurement procedure. With this method, an average target thickness of 14 μm was achieved, allowing to consider the beam energy constant within the uncertainties over the full irradiated mass.

Each target was then irradiated with a proton beam with a flat surface distribution, so that any inhomogeneities in thickness due to sedimentation could be neglected. This procedure, successfully used in our previous work on cross section measurements (Carzaniga and Braccini, 2019; Dellepiane et al., 2022a; Braccini et al., 2022; Dellepiane et al., 2022d), is described in detail in Carzaniga et al. (2017).

The beam was flattened by the optical elements of the BTL and monitored online with the UniBEaM detector. A custom target station, providing a controlled diameter beam thanks to an 8-mm collimator, was connected to an electrometer (B2985A Keysight) and used to measure the beam current hitting the target. An electron suppressor ring connected to a negative bias voltage is embedded in the station to repel secondary electrons produced during the irradiation, that would increase the measured current. To perform irradiations below 18 MeV, the beam energy was degraded by means of aluminum attenuator disks placed in front of the target and was determined using the SRIM-2013 Monte Carlo code (Ziegler and Manoyan, 2013).

The average irradiation time in each run was 7 min and the beam current about 11 nA. After the End of Beam (EOB), the produced activity was measured by γ spectrometry with the HPGe detector. In all measurements, the count frequency was sufficiently low to limit negative effects due to pile up (dead time below 1%).

During the irradiation, ^{67}Ga is also produced from the secondary reactions ^{67}Zn(p,n)^{67}Ga and ^{68}Zn(p,2n)^{67}Ga, which occurs on the 0.02% ^{67}Zn and 1.20% ^{68}Zn, respectively, present as impurities in the enriched ^{70}ZnO material used in this work (Table 3). All the γ-lines emitted in the decay of ^{67}Cu are also observed in the decay of ^{67}Ga. As the half-life of ^{67}Ga is 3.26 d and the half-life of ^{67}Cu is 2.58 d, ^{67}Ga cannot be removed from the sample by means of decay time. For this reason, a method based on the inversion of a linear system of equations was applied to disentangle the two contributions.

By irradiating a sample at the proton energy E and by measuring the count rates $\rho(t)$ of the two common peaks at 93.3 keV and 184.6 keV (Table 2), the following linear system holds:

$$\begin{cases} \rho_{93}(t) = \sum_k A_k(t_0) \cdot BR_{k,93} \cdot \epsilon_{93} \cdot f_k \cdot e^{-\lambda_k t} \\ \rho_{185}(t) = \sum_k A_k(t_0) \cdot BR_{k,185} \cdot \epsilon_{185} \cdot f_k \cdot e^{-\lambda_k t} \end{cases} \quad (1)$$

where k =^{67}Cu, ^{67}Ga, $A_k(t_0)$ is the EOB activity to be determined, ϵ is the HPGe efficiency for the given peak energy, BR_k is the branching ratio of the kth radionuclide referred to the given peak, $f_k = \frac{1 - e^{-\lambda_k \cdot RT}}{\lambda_k \cdot RT}$ and $e^{-\lambda_k t}$ are the correction factors for the measurement duration and the cooling time, respectively, with λ_k the decay constant of the kth radionuclide and RT the real time of the measurement.

The solution of the linear system allows to determine the EOB activity of the two radionuclides, from which the cross sections dependence on the proton energy E can be calculated as

$$\sigma(E) = A(t_0) \cdot \frac{q}{\tilde{I}} \cdot \frac{1}{m \cdot \frac{N_A \epsilon \eta}{m_{mol}}} \cdot \frac{1}{1 - e^{-\lambda t_i}} \quad (2)$$

where q is the elementary charge, $\tilde{I}$ the current per unit surface, m the mass of the irradiated target, N_A the Avogadro constant, m_{mol} the molecular mass of the target material, ϵ the isotopic ratio of the target nucleus, η its stoichiometric number and t_i the irradiation time.

2.3. Study of ^{67}Cu production yield and purity

Aiming at an optimized production of ^{67}Cu, a study of the Thick Target Yield (TTY) and of the purity was performed. From the cross

section measurements, the TTY as a function of the proton energy on target E can be calculated using the following formula

$$TTY(E) = \frac{A(t_i)}{I \cdot t_i} = \frac{(1 - e^{-\lambda \cdot t_i})}{m_{mol} \cdot q} \int_{E_{th}}^{E} \frac{\sigma(E')}{S_p(E')} dE' \quad (3)$$

where $(1 - e^{-\lambda \cdot t_i})$ is the Saturation Factor (SF), with t_i the irradiation time and λ the decay constant, I the current on target, $A(t_i)$ the activity produced at EOB, $\sigma(E')$ the cross section as a function of the proton kinetic energy E', $S_p(E')$ is the mass stopping power for the target material, E_{th} is the threshold energy of the considered reaction, N_A the Avogadro constant, m_{mol} the average molar mass of the target material, η the number of target atoms of the desired species per molecule and q the charge of the projectile. The mass stopping power was calculated using SRIM.

Given a sample containing a mixture of N radioisotopes, the purity of the radionuclide of interest X is given by

$$P_X = \frac{A_X}{\sum_i^N A_i} \quad (4)$$

where A_i is the activity of the ith radionuclide.

If a thin target is used, so that the protons are not stopped therein, the production yield, Y(E), can be defined as

$$Y(E) = TTY(E) - TTY(E_{out}) \quad (5)$$

where E_{out} is the proton energy after the target, calculated by using SRIM.

2.4. ^{67}Cu production tests

The target used for the production tests was prepared by compressing approximately 58 mg of enriched ^{70}ZnO powder, with the application of an axial force of about 4 $\cdot 10^4$ N. The thickness of the obtained 6-mm-diameter disk-shaped pellet could not be measured due to its high fragility and was therefore calculated on the basis of the theoretical density of ZnO (5.61 g/cm^3 (National Center for Biotechnology Information, 2022)), resulting in ca. 366 μm.

The pellet was placed in a special capsule – called coin – designed and built by our group and successfully used to produce several radionuclides (Dellepiane et al., 2022b,a; Braccini et al., 2022; van der Meulen et al., 2020; Favaretto et al., 2021). The coin is composed by two aluminum halves, the lid and the cup, kept together by small permanent magnets, as shown in Fig. 2-a. The cup hosts the 6-mm-diameter pellet and an O-ring to prevent the leakage of possible molten material or of any gas produced during the irradiation. To optimize the ^{67}Cu production yield and purity, the energy of the protons reaching the target material was set by adjusting the thickness of the lid. In particular, a lid with a 7-mm-diameter hole (Fig. 2-b) was used in some production tests in order not to degrade the beam energy. In this case, a 14-mm-diameter and 13-μm-thick aluminum disk was placed inside the coin to prevent possible pellet leakage (Fig. 2-c). The O-ring ensures that the aluminum disk stays in place during the irradiation.

The current was measured throughout each irradiation by connecting the body of the STS to the B2985A Keysight electrometer. The effective current hitting the pellet was assessed by measuring the 2D beam profiles with radiochromic films (Casolaro, 2021) and it was measured within an uncertainty of 10%.

3. Experimental results

3.1. Cross section measurements

The results of the ^{70}Zn(p,α)^{67}Cu cross section measurements, obtained from Eqs. (1) and (2), are presented in Fig. 3; for completeness, the numerical values are reported in the Appendix (Table 5). Our measurements are in good agreement with the data available in the literature (Kastleiner et al., 1999; Levkowskij, 1991). In accordance with

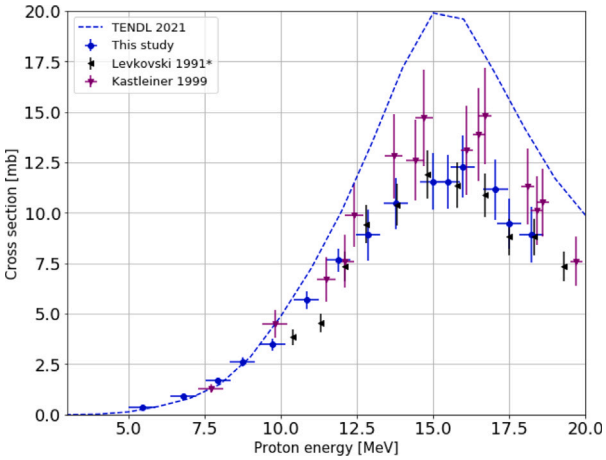

Fig. 3. ^{70}Zn(p,α)^{67}Cu nuclear cross section.

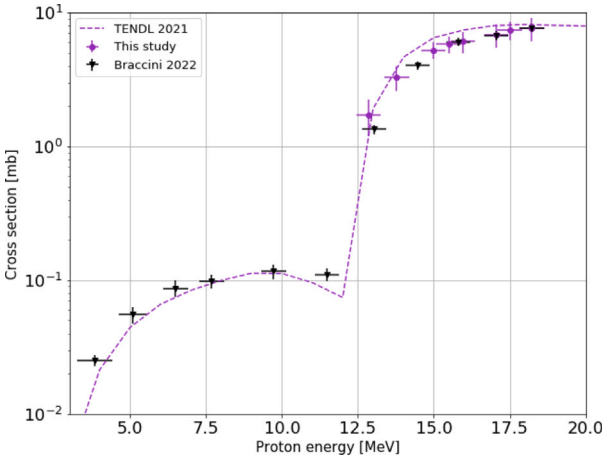

Fig. 4. ^{67}Ga production cross sections.

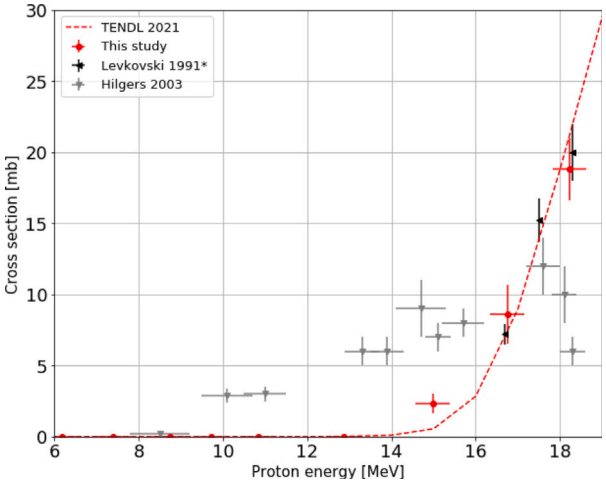

Fig. 5. ^{68}Zn(p,αn)^{64}Cu nuclear cross sections.

the findings of Takács et al. (2002), the values presented in Levkowskij (1991) were scaled by a factor of 0.8, on the basis of the currently accepted value of the monitor reaction that was used by Levkovski in his original work. TENDL-2021 calculation (Koning and Rochman, 2012) predicts the same peak position but it overestimates the cross section values over the entire excitation function curve for energies above 10 MeV.^{67}Ga is produced from ^{67}Zn and ^{68}Zn via the reactions ^{67}Zn(p,n)^{67}Ga and ^{68}Zn(p,2n)^{67}Ga, respectively. The ^{67}Ga production

cross sections were measured to test the linear system method and are shown in Fig. 4 together with our previous findings (Braccini et al., 2022), normalized by the isotopic abundance of ^{67}Zn and ^{68}Zn, present in the enriched ^{70}ZnO used in this study.

The numerical data are reported in the Appendix (Table 6). A good agreement was found for energies above 12 MeV, corresponding to the cross section measurements of the ^{68}Zn(p,2n)^{67}Ga reaction. As for the ^{67}Zn(p,n)^{67}Ga reaction, its cross section could not be measured in this study because of the low percentage of ^{67}Zn in the target material. According to TENDL-2021, ^{64}Cu should also be produced in the energy range of interest via the ^{67}Zn(p,α)^{64}Cu and ^{68}Zn(p,αn)^{64}Cu reactions. However, due to the low isotopic abundance of ^{67}Zn and ^{68}Zn in the enriched ^{70}Zn material (0.02% and 1.20%, respectively) and the low intensity of the γ-emission (Table 2), it was not possible to detect ^{64}Cu by irradiating enriched ^{70}ZnO samples.

The ^{68}Zn(p,αn)^{64}Cu nuclear reaction cross section was measured by irradiating enriched ^{68}Zn foils, whose isotopic composition is reported in Table 3. The results are presented in Fig. 5; for completeness, the numerical values are reported in the Appendix (Table 7). Our measurements are in agreement with TENDL-2021 calculations and with the experimental data reported by Levkowskij (1991) (corrected according to Takács et al. (2002)). The data reported by Hilgers et al. (2003) differ considerably from both this study and TENDL predictions.

As for the ^{67}Zn(p,α)^{64}Cu nuclear reaction, its cross section was measured in the framework of our research program on Cu radioisotopes from 89.6% enriched ^{67}ZnO targets (Dellepiane et al., 2022c) (^{64}Zn: 1.56%; ^{66}Zn: 3.88%; ^{67}Zn: 89.60%; ^{68}Zn: 4.91%; ^{70}Zn: 0.05%) .

3.2. Production tests

The thick target yield of ^{67}Cu and ^{64}Cu were calculated from Eq. (3) on the basis of the cross section measurements reported in this paper and in Dellepiane et al. (2022c) and are shown in Fig. 6 as a function of the entry energy. The irradiation time t_i is set to 1 h.

The fraction of ^{67}Cu produced and the presence of the main impurity ^{64}Cu depend on the energy of the proton beam entering the target, as shown in Fig. 7, where the radionuclidic purity is calculated according to Eq. (4). In particular, the highest ^{67}Cu production yield can be reached irradiating the target with the maximum achievable energy, while the radionuclidic purity rapidly decreases after 14 MeV due to the ^{68}Zn(p,αn)^{64}Cu reaction.

Since the main impurity is ^{64}Cu and its half-life is much shorter than that of ^{67}Cu, the radionuclidic purity can be improved considering longer irradiation times and/or letting the target decay after EoB. It is important to remark that ^{64}Cu is also a β^- emitter and contributes to the dose to the patient.

Irradiating a 98.75% enriched ^{70}ZnO thick target with the maximum reachable energy of 17.8 MeV, a ^{67}Cu TTY of 154 MBq/μA can be achieved at saturation with a radionuclidic purity of 99.5%. Radionuclidic purity further improves during the chemical processing time between the EoB and the application to patients, because of the decay of ^{64}Cu. However, it is important to remark that, in order to have a high labeling efficiency, also the non-radioactive impurities produced during the irradiation have to be carefully evaluated and, if necessary, reduced to avoid interference with ^{67}Cu in the radiolabelling procedure.

To confirm these predictions based on cross section measurements, two production tests were performed in the energy range (17.8–15.8) MeV by irradiating the 0.37-mm-thick enriched ^{70}ZnO pellet with the solid target station. To reach a higher energy, a third test was carried out at the BTL, by means of an adapted version of the station used for cross section measurements. The energy ranges, the irradiation parameters and the activities are reported in Table 4. Fig. 8 shows the experimental results compared with the production yields (Eq. (5)) and the radionuclidic purity calculated from our cross section measurements under irradiation conditions. In the first two productions, ^{64}Cu could not be measured with the HPGe detector and the experimental purity was overestimated. In the last test, a good agreement was found.

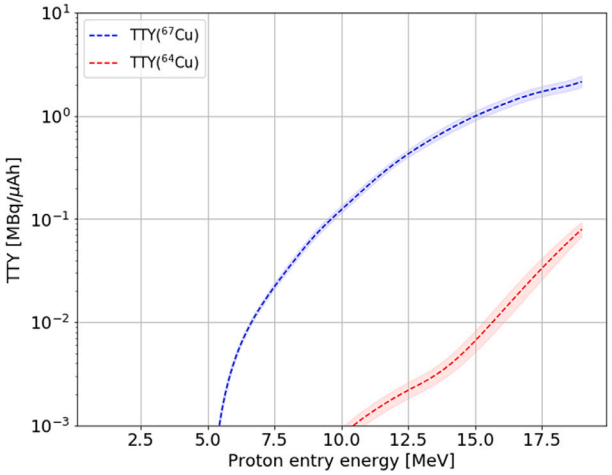

Fig. 6. ^{67}Cu and ^{64}Cu thick target yields as a function of the entry energy for a 98.75% enriched ^{70}ZnO target. The irradiation time is set to 1 h. The bands correspond to the maximum and minimum yield calculated on the basis of the measured cross sections.

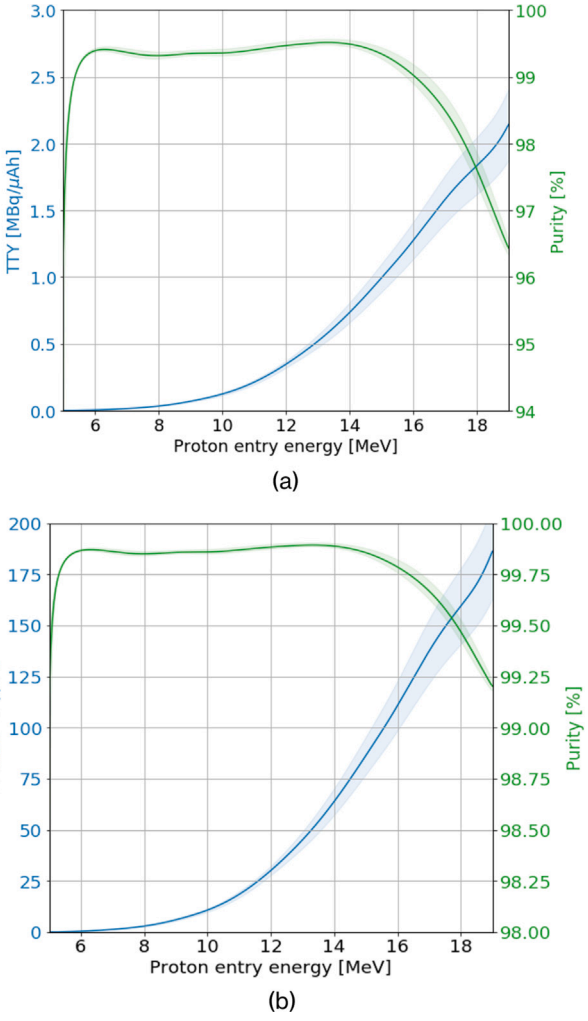

Fig. 7. ^{67}Cu thick target yield and purity at EOB for a 98.75% enriched ^{70}ZnO target, considering an irradiation time of 1 h (a) and at saturation (b). The bands correspond to the maximum and minimum yield calculated on the basis of the measured cross sections.

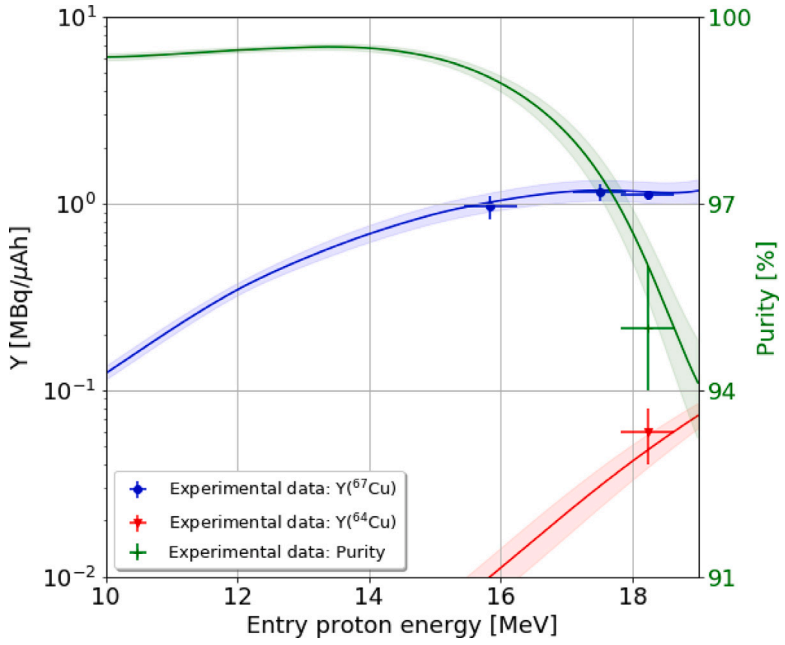

Fig. 8. ^{67}Cu and ^{64}Cu yields and radionuclidic purity calculated from the measured cross section in our irradiation conditions compared to the experimental results. The bands correspond to the maximum and minimum yield calculated on the basis of the measured cross sections.

Table 4
Irradiation parameters, ^{67}Cu and ^{64}Cu yields and radionuclidic purity at EOB obtained irradiating the 0.37-mm-thick 98.75% enriched ^{70}ZnO pellet. The values in parentheses are the yield calculations based on the cross section measurements.

E_{in} [MeV]	E_{out} [MeV]	t_i [min]	I [nA]	Q $\cdot 10^{-3}$ [μAh]	Y(^{67}Cu) [MBq/μAh]	Y(^{64}Cu) [MBq/μAh]	P(EoB) [%]
15.8 ± 0.4	11.0 ± 0.4	~ 9	52.7 ± 0.5	7.9 ± 0.8	0.96 ± 0.14 *(1.02)*	No Signal *(0.01)*	Compatible with 100 *(99)*
17.5 ± 0.4	13.2 ± 0.4	~ 30	3.44 ± 0.03	1.7 ± 0.2	1.15 ± 0.12 *(1.18)*	No Signal *(0.03)*	Compatible with 100 *(98)*
18.2 ± 0.4	14.0 ± 0.4	~ 79	28.7 ± 0.3	37.7 ± 1.8	1.11 ± 0.07 *(1.15)*	0.06 ± 0.02 *(0.05)*	95 ± 1 *(96)*

4. Conclusions and outlook

The aim of this study was to investigate the feasibility of ^{67}Cu production with a medical cyclotron, irradiating an enriched ^{70}ZnO solid target with an 18 MeV proton beam. To select the optimal irradiation conditions, the cross sections of the nuclear reactions involved were measured at the Bern medical cyclotron laboratory. In particular, the ^{70}Zn(p,α)^{67}Cu and the ^{68}Zn(p,αn)^{64}Cu nuclear cross section were measured from enriched ^{70}ZnO and enriched ^{68}Zn samples, respectively. The latter was of paramount importance to quantify the co-production of ^{64}Cu during the irradiation, which represents the only copper impurity in the sample.

Several production tests were successfully performed irradiating a 98.75% enriched ^{70}ZnO pellet with a solid target station to confirm the cross section measurement results. To the best of our knowledge, this was the first time that ^{64}Cu has been experimentally measured in the production route and energy range investigated, considered impurity-free for energies above 23 MeV and for 100% ^{70}Zn enriched targets (Mou et al., 2022). However, since ^{64}Cu presents a much shorter half-life than ^{67}Cu, its quantity can be minimized by considering long irradiation times and letting the target decay after EoB. In particular, a thick target yield of 154 MBq/μA with a radionuclidic purity of 99.5% can be achieved at saturation for an entry energy of 17.8 MeV. The radionuclidic purity further increases during the time required for radiochemical processing.

Although the ^{67}Cu production yield is rather low, modern medical cyclotrons are capable of delivering high beam currents (above 300 μA), making it possible to obtain sufficient quantities of ^{67}Cu with the radionuclidic purity required for nuclear medicine applications. In this respect, is important to note that the dose of ^{67}Cu radioactivity required for one treatment is about 3.7 GBq (IAEA-TECDOC-1340, 2003).

The results achieved in this study confirm the predictions reported by Kastleiner et al. (1999) and represent an important step forward towards the use of medical cyclotrons for the production of ^{67}Cu for applications in theranostics.

CRediT authorship contribution statement

Gaia Dellepiane: Writing – review & editing, Writing – original draft, Validation, Software, Methodology, Investigation, Formal analysis, Data curation, Conceptualization. **Pierluigi Casolaro:** Writing – review & editing, Investigation, Conceptualization. **Alexander Gottstein:** Writing – review & editing, Investigation. **Isidre Mateu:** Writing – review & editing, Investigation, Conceptualization. **Paola Scampoli:** Writing – review & editing, Investigation. **Saverio Braccini:** Writing – review & editing, Supervision, Resources, Project administration, Methodology, Investigation, Funding acquisition, Conceptualization.

Declaration of competing interest

The authors declare the following financial interests/personal relationships which may be considered as potential competing interests: Saverio Braccini reports financial support was provided by Swiss National Science Foundation.

Data availability

Data will be made available on request.

Acknowledgments

We acknowledge contributions from LHEP engineering and technical staff (Roger Hänni and Jan Christen, in particular) and from the SWAN Isotopen AG team (Riccardo Bosi and Michel Eggemann, in particular). This research project was partially funded by the Swiss National Science Foundation (SNSF) (grants: CRSII5_180352 and 200021_175749).

Appendix

See Tables 5–7.

Table 5
^{70}Zn(p,α)^{67}Cu nuclear cross section data.

E [MeV]	^{70}Zn(p,α)^{67}Cu [mbarn]
5.5 ± 0.4	0.36 ± 0.03
6.8 ± 0.4	0.92 ± 0.06
7.9 ± 0.4	1.7 ± 0.1
8.7 ± 0.4	2.6 ± 0.2
9.7 ± 0.4	3.5 ± 0.3
10.8 ± 0.4	5.7 ± 0.4
11.9 ± 0.4	7.6 ± 0.6
12.9 ± 0.4	8.9 ± 1.3
13.8 ± 0.4	10.5 ± 1.3
15.0 ± 0.4	11.6 ± 1.4
15.5 ± 0.4	11.5 ± 1.4
16.0 ± 0.4	12.3 ± 1.5
17.1 ± 0.4	11.2 ± 1.5
17.5 ± 0.4	9.5 ± 1.3
18.2 ± 0.4	8.9 ± 1.4

Table 6
^{67}Ga production cross section data, measured irradiating the 98.75% enriched ^{70}ZnO material (Table 3).

E [MeV]	^{70}Zn(p,x)^{67}Ga [mbarn]
5.5 ± 0.4	No Signal
6.8 ± 0.4	No Signal
7.9 ± 0.4	No Signal
8.7 ± 0.4	No Signal
9.7 ± 0.4	No Signal
10.8 ± 0.4	No Signal
11.9 ± 0.4	No Signal
12.9 ± 0.4	1.7 ± 0.5
13.8 ± 0.4	3.3 ± 0.7
15.0 ± 0.4	5.2 ± 0.7
15.5 ± 0.4	5.8 ± 0.8
16.0 ± 0.4	6.1 ± 1.1
17.1 ± 0.4	6.8 ± 1.3
17.5 ± 0.4	7.3 ± 1.1
18.2 ± 0.4	7.6 ± 1.5

Table 7
^{68}Zn(p,αn)^{64}Cu nuclear cross section data.

E [MeV]	^{68}Zn(p,αn)^{64}Cu [mbarn]
15.0 ± 0.4	2.3 ± 0.7
16.8 ± 0.4	8.6 ± 2.0
18.2 ± 0.4	18.8 ± 2.2

References

Aliev, R.A., Belyshev, S.S., Kuznetsov, A.A., Dzhilavyan, L.Z., Khankin, V.V., Aleshin, G.Y., Kazakov, A.G., Priselkova, A.B., Kalmykov, S.N., Ishkhanov, B.S., 2019. Photonuclear production and radiochemical separation of medically relevant radionuclides: ^{67}Cu. J. Radioanal. Nucl. Chem. 321, 125–132. http://dx.doi.org/10.1007/s10967-019-06576-9.

Auger, M., Braccini, S., Carzaniga, T.S., Ereditato, A., Nesteruk, K.P., Scampoli, P., 2016. A detector based on silica fibers for ion beam monitoring in a wide current range. J. Instrum. 11 (03), P03027. http://dx.doi.org/10.1088/1748-0221/11/03/p03027.

Auger, M., Braccini, S., Ereditato, A., Nesteruk, K.P., Scampoli, P., 2015. Low current performance of the bern medical cyclotron down to the pa range. Meas. Sci. Technol. 26, http://dx.doi.org/10.1088/0957-0233/26/9/094006.

Bhike, M., Saxena, A., Roy, B.J., Choudhury, R.K., Kailas, S., Ganesan, S., 2009. Measurement of ^{67}Zn(n,p)^{67}Cu, ^{92}Mo(n,p)^{92m}Nb, and ^{98}Mo(n,γ)^{99}Mo reaction cross sections at incident neutron energies of En=1.6 and 3.7 MeV. Nucl. Sci. Eng. 163 (2), 175–182. http://dx.doi.org/10.13182/NSE163-175.

Braccini, S., 2013. The new bern PET cyclotron, its research beam line, and the development of an innovative beam monitor detector. AIP Conf. Proc. 1525, 144–150. http://dx.doi.org/10.1063/1.4802308.

Braccini, S., Carzaniga, T.S., Dellepiane, G., Grundler, P.V., Scampoli, P., van der Meulen, N.P., Wüthrich, D., 2022. Optimization of ^{68}Ga production at an 18 MeV medical cyclotron with solid targets by means of cross-section measurement of ^{66}Ga, ^{67}Ga and ^{68}Ga. Appl. Radiat. Isot. 110252. http://dx.doi.org/10.1016/j.apradiso.2022.110252.

Braccini, S., Scampoli, P., 2016. Science with a medical cyclotron. CERN Courier 21–22.

Carzaniga, T.S., Auger, M., Braccini, S., Bunka, M., Ereditato, A., Nesteruk, K.P., Scampoli, P., Türler, A., van der Meulen, N., 2017. Measurement of ^{43}Sc and ^{44}Sc production cross-section with an 18 MeV medical PET cyclotron. Appl. Radiat. Isot. 129, 96–102. http://dx.doi.org/10.1016/j.apradiso.2017.08.013.

Carzaniga, T.S., Braccini, S., 2019. Cross-section measurement of ^{44m}Sc, ^{47}Sc, ^{48}Sc and ^{47}Ca for an optimized ^{47}Sc production with an 18 MeV medical PET cyclotron. Appl. Radiat. Isot. 143, 18–23. http://dx.doi.org/10.1016/j.apradiso.2018.10.015.

Casolaro, P., 2021. Radiochromic films for the two-dimensional dose distribution assessment. Appl. Sci. 11 (5), http://dx.doi.org/10.3390/app11052132.

Champion, C., Quinto, M.A., Morgat, C., Zanotti-Fregonara, P., Hindié, E., 2016. Comparison between three promising β^--emitting radionuclides, ^{67}Cu, ^{47}Sc and ^{161}Tb, with emphasis on doses delivered to minimal residual disease. Theranostics 6 (10), 1611–1618. http://dx.doi.org/10.7150/thno.15132.

Chen, J., Jiang, Y., Shi, H., Peng, Y., Fan, X., Li, C., 2020. The molecular mechanisms of copper metabolism and its roles in human diseases. Eur. J. Physiol. 472, 1415–1429. http://dx.doi.org/10.1007/s00424-020-02412-2.

Cortecnet, 2022. URL https://cortecnet.com/ (Accessed 14 October 2022).

Dehnel, M., Potkins, D., Stewart, T., 2013. An integrated self-supporting mini-beamline for PET cyclotrons. In: Proceedings of CYC2013, Vancouver, BC, Canada.

Dellepiane, G., Casolaro, P., Favaretto, C., Grundler, P.V., Mateu, I., Scampoli, P., Talip, Z., van der Meulen, N.P., Braccini, S., 2022a. Cross section measurement of terbium radioisotopes for an optimized ^{155}Tb production with an 18 MeV medical PET cyclotron. Appl. Radiat. Isot. 184, 110175. http://dx.doi.org/10.1016/j.apradiso.2022.110175.

Dellepiane, G., Casolaro, P., Häffner, P., Mateu, I., Scampoli, P., Voeten, N., Zyaee, E., Braccini, S., 2022b. New methods for theranostic radioisotope production with solid targets at the bern medical cyclotron. EPJ Web Conf. 261, 05006. http://dx.doi.org/10.1051/epjconf/202226105006.

Dellepiane, G., Casolaro, P., Mateu, I., Scampoli, P., Braccini, S., 2022c. Alternative routes for ^{64}Cu production using an 18 MeV medical cyclotron in view of theranostic applications. Appl. Radiat. Isot. 110518. http://dx.doi.org/10.1016/j.apradiso.2022.110518.

Dellepiane, G., Casolaro, P., Mateu, I., Scampoli, P., Voeten, N., Braccini, S., 2022d. ^{47}Sc and ^{46}Sc cross-section measurement for an optimized ^{47}Sc production with an 18 MeV medical PET cyclotron. Appl. Radiat. Isot. 189, 110428, 1872-9800.

Dellepiane, G., Casolaro, P., Mateu, I., Scampoli, P., Voeten, N., Braccini, S., 2022e. Cross-section measurement for an optimized ^{61}Cu production at an 18 MeV medical cyclotron from natural Zn and enriched ^{64}Zn solid targets. Appl. Radiat. Isot. 190, 110466. http://dx.doi.org/10.1016/j.apradiso.2022.110466.

Favaretto, C., Talip, Z., Borgna, F., Grundler, P.V., Dellepiane, G., Sommerhalder, A., Zhang, H., Schibli, R., Braccini, S., Müller, C., van der Meulen, N.P., 2021. Cyclotron production and radiochemical purification of terbium-155 for SPECT imaging. EJNMMI Radiopharmacy Chem. 6, 37. http://dx.doi.org/10.1186/s41181-021-00153-w.

Forgács, A., Balkay, L., Trón, L., Raics, P., 2014. Excel2Genie: A microsoft excel application to improve the flexibility of the genie-2000 spectroscopic software. Appl. Radiat. Isot. 94, 77–81. http://dx.doi.org/10.1016/j.apradiso.2014.07.005.

Furuta, M., Shimizu, T., Hayashi, H., Miyazaki, I., Yamamoto, H., Shibata, M., Kawade, K., 2008. Measurements of activation cross sections of (n,p) and (n,α) reactions in the energy range of 3.5–5.9 MeV using a deuterium gas target. Ann. Nucl. Energy 35 (9), 1652–1662. http://dx.doi.org/10.1016/j.anucene.2008.02.010.

Häffner, P.D., Aguilar, C.B., Braccini, S., Scampoli, P., Thonet, P.A., 2019. Study of the extracted beam energy as a function of operational parameters of a medical cyclotron. Instruments 3 (63), http://dx.doi.org/10.3390/instruments3040063.

Häffner, P.D., Belver-Aguilar, C., Casolaro, P., Dellepiane, G., Scampoli, P., Braccini, S., 2021. An active irradiation system with automatic beam positioning and focusing for a medical cyclotron. Appl. Sci. 11 (6), http://dx.doi.org/10.3390/app11062452.

Hilgers, K., Stoll, T., Skakun, Y., Coenen, H., Qaim, S., 2003. Cross-section measurements of the nuclear reactions ^{nat}Zn(d,x)^{64}Cu, ^{66}Zn(d,α)^{64}Cu and ^{68}Zn(p,αn)^{64}Cu for production of ^{64}Cu and technical developments for small-scale production of ^{67}Cu via the ^{70}Zn(p,α)^{67}Cu process. Appl. Radiat. Isot. 59 (5), 343–351. http://dx.doi.org/10.1016/S0969-8043(03)00199-4.

Hovhannisyan, G., Bakhshiyan, T., Dallakyan, R., 2021. Photonuclear production of the medical isotope ^{67}Cu. Nucl. Instrum. Methods Phys. Res. B 498, 48–51. http://dx.doi.org/10.1016/j.nimb.2021.04.016.

IAEA, 2016. Cyclotron Produced Radionuclides: Emerging Positron Emitters for Medical Applications: ^{64}Cu and ^{124}I. IAEA Radioisotopes and Radiopharmaceutical Reports No. 1, Vienna.

IAEA, 2022. Live chart of nuclides, available online. URL https://nds.iaea.org/relnsd/vcharthtml/VChartHTML.html (Accessed 08 April 2022).

IAEA-TECDOC-1340, 2003. Manual for reactor produced radioisotope. Vienna: Int. Atomic Energy Agency 1–254.

International Standard, 2021. Nuclear Instrumentation – Measurement of Activity Or Emission Rate of Gamma-Ray Emitting Radionuclides – Calibration and Use of Germanium-Based Spectrometers. IEC 61452:2021.

Isoflex, 2022. Isotope for science, medicine and industry. URL http://www.isoflex.com/ (Accessed 14 October 2022).

Johnsen, A., Heidrich, B., Durrant, C., et al., 2015. Reactor production of ^{64}Cu and ^{67}Cu using enriched zinc target material. J. Radioanal. Nucl. Chem. 305, 61—71. http://dx.doi.org/10.1007/s10967-015-4032-6.

Kastleiner, S., Coenen, H., Qaim, S., 1999. Possibility of production of ^{67}Cu at a small-sized cyclotron via the (p,alpha)-reaction on enriched ^{70}Zn. Radiochim. Acta 84, 107–110.

Kielan, D., Marcinkowski, A., 1995. Cross sections for (n, p) reaction on zinc isotopes in terms of the novel multistep compound reaction model. Z. Phys. A Hadrons Nucl. 352, 137–143. http://dx.doi.org/10.1007/BF01298899.

Koning, A., Rochman, D., 2012. Modern Nuclear Data Evaluation With The TALYS Code System. Nucl. Data Sheets 113, 1934–2841. http://dx.doi.org/10.1016/j.nds.2012.11.002.

Kozempel, J., Abbas, K., Simonelli, F., Bulgheroni, A., Holzwarth, U., Gibson, N., 2012. Preparation of ^{67}Cu via deuteron irradiation of ^{70}Zn. Radiochim. Acta 100 (7), 419–424. http://dx.doi.org/10.1524/ract.2012.1939.

Levkowskij, V., 1991. Activation cross sections for the nuclides of Medium Mass Region (A=40-100) with protons and α-particles at medium (E=10-50 MeV) energies. Inter-Vesti, Moscow.

McGee, T., Rao, C., Saha, G., Yaffe, L., 1970. Nuclear interactions of ^{45}Sc and ^{68}Zn with protons of medium energy. Nuclear Phys. A 150 (1), 11–29. http://dx.doi.org/10.1016/0375-9474(70)90451-3.

Merrick, M.J., Rotsch, D.A., Tiwari, A., Nolen, J., Brossard, T., Song, J., Wadas, T.J., Sunderland, J.J., Graves, S.A., 2021. Imaging and dosimetric characteristics of ^{67}Cu. Phys. Med. Amp: Biol. 66 (3), 035002. http://dx.doi.org/10.1088/1361-6560/abca52.

van der Meulen, N.P., Hasler, R., Talip, Z., Grundler, P.V., Favaretto, C., Umbricht, C.A., Müller, C., Dellepiane, G., Carzaniga, T.S., Braccini, S., 2020. Developments toward the implementation of ^{44}Sc production at a medical cyclotron. Molecules 25 (20), http://dx.doi.org/10.3390/molecules25204706.

Mirion Technologies, 2022. GENIE 2000 - basic spectroscopy software. URL https://www.mirion.com/products/genie-2000-basic-spectroscopy-software (Accessed 12 October 2022).

Morrison, D.L., Caretto, A.A., 1962. Excitation functions of (p, xp) reactions. Phys. Rev. 127, 1731–1738. http://dx.doi.org/10.1103/PhysRev.127.1731.

Morrison, D.L., Caretto, A.A., 1964. Recoil study of the ^{68}Zn(p,2p)^{67}Cu reaction. Phys. Rev. 133, B1165–B1170. http://dx.doi.org/10.1103/PhysRev.133.B1165.

Mou, L., Martini, P., Pupillo, G., Cieszykowska, I., Cutler, C.S., Mikołajczak, R., 2022. ^{67}Cu production capabilities: A mini review. Molecules 27, 1501. http://dx.doi.org/10.3390/molecules27051501.

Mou, L., Pupillo, G., Martini, P., Pasquali, M., 2021. A method and a target for the production of ^{67}Cu. European Patent EP3794615.

National Center for Biotechnology Information, 2022. PubChem compound summary. URL https://pubchem.ncbi.nlm.nih.gov (Accessed 02 August 2022).

Nesaraja, C., Linse, K.-H., Spellerberg, S., Sudar, S., Suhaimi, A., Qaim, S.M., 1999. Excitation functions of neutron induced reactions on some isotopes of zinc, gallium and germanium in the energy range of 6.2 to 12.4 MeV. Radiochim. Acta 86 (1–2), 1–10. http://dx.doi.org/10.1524/ract.1999.86.12.1.

Nesteruk, K.P., Auger, M., Braccini, S., Carzaniga, T.S., Ereditato, A., Scampoli, P., 2018. A system for online beam emittance measurements and proton beam characterization. J. Instrum. 13, P01011. http://dx.doi.org/10.1088/1748-0221/13/01/p01011.

Nigron, E., Guertin, A., Haddad, F., Sounalet, T., 2021. Is ^{70}Zn(d,x)^{67}Cu the best way to produce ^{67}Cu for medical applications? Front. Med. 8, http://dx.doi.org/10.3389/fmed.2021.674617.

Potkins, D.E., Braccini, S., Nesteruk, K.P., Carzaniga, T.S., Vedda, A., Chiodini, N., Timmermans, J., Melanson, S., Dehnel, M.P., 2017. A low-cost beam profiler based on cerium-doped silica fibers. In: Proceedings of CAARI-16, Physics Procedia. http://dx.doi.org/10.1016/j.phpro.2017.09.061.

Pupillo, G., Mou, L., Martini, P., Pasquali, M., Boschi, A., Cicoria, G., Duatti, A., Haddad, F., Esposito, J., 2020. Production of ^{67}Cu by enriched ^{70}Zn targets: first measurements of formation cross sections of ^{67}Cu, ^{64}Cu, ^{67}Ga, ^{66}Ga, ^{69m}Zn and ^{65}Zn in interactions of ^{70}Zn with protons above 45 MeV. Radiochim. Acta 108 (8), 593–602. http://dx.doi.org/10.1515/ract-2019-3199.

Pupillo, G., Sounalet, T., Michel, N., Mou, L., Esposito, J., Haddad, F., 2018. New production cross sections for the theranostic radionuclide ^{67}Cu. Nucl. Instrum. Methods Phys. Res. B 415, 41–47. http://dx.doi.org/10.1016/j.nimb.2017.10.022.

Sandia National Laboratories, 2022. InterSpec - spectral radiation analysis software. URL https://sandialabs.github.io/InterSpec/ (Accessed 12 October 2022).

Schwarzbach, R., Zimmermann, K., Novak-Hofer, I., Schubiger, P.A., 2001. A comparison of ^{67}Cu production by proton (67 TO 12 MeV) induced reactions on ^{nat}Zn and on enriched ^{68}ZN/^{70}ZN. J. Label. Compounds Radiopharmaceuticals 44 (S1), S809–S811. http://dx.doi.org/10.1002/jlcr.25804401284.

Shimizu, T., Sakane, H., Shibata, M., Kawade, K., Nishitani, T., 2004. Measurements of activation cross sections of (n,p) and (n,α) reactions with d-D neutrons in the energy range of 2.1–3.1 MeV. Ann. Nucl. Energy 31 (9), 975–990. http://dx.doi.org/10.1016/j.anucene.2003.12.005.

Skakun, Y., Qaim, S., 2004. Excitation function of the ^{64}Ni(α,p)^{67}Cu reaction for production of ^{67}Cu. Appl. Radiat. Isot. 60 (1), 33–39. http://dx.doi.org/10.1016/j.apradiso.2003.09.003.

Starovoitova, V., Foote, D., Harris, J., Makarashvili, V., Segebade, C.R., Sinha, V., Wells, D.P., 2011. ^{67}Cu photonuclear production. AIP Conf. Proc. 1336, 189–196. http://dx.doi.org/10.1063/1.3586150.

Stoll, T., Kastleiner, S., Shubin, Y.N., Coenen, H.H., Qaim, S.M., 2002. Excitation functions of proton induced reactions on ^{68}Zn from threshold up to 71 MeV, with specific reference to the production of ^{67}Cu. Radiochim. Acta 90 (6), 309–313. http://dx.doi.org/10.1524/ract.2002.90.6.309.

Szelecsényi, F., Steyn, G., Dolley, S., Kovács, Z., Vermeulen, C., van der Walt, T., 2009. Investigation of the ^{68}Zn(p, 2p)^{67}Cu nuclear reaction: New measurements up to 40 MeV and compilation up to 100 MeV. Nucl. Instrum. Methods Phys. Res. Section B-Beam Interact. Mater. Atoms 267, 1877–1881. http://dx.doi.org/10.1016/j.nimb.2009.03.097.

Takács, S., Aikawa, M., Haba, H., Komori, Y., Ditrói, F., Szücs, Z., Saito, M., Murata, T., Sakaguchi, M., Ukon, N., 2020. Cross sections of alpha-particle induced reactions on ^{nat}Ni: Production of ^{67}Cu. Nucl. Instrum. Methods Phys. Res. B 479, 125–136. http://dx.doi.org/10.1016/j.nimb.2020.06.022.

Takács, S., Tárkányi, F., Sonck, M., Hermanne, A., 2002. Investigation of the ^{nat}Mo(p,x)^{96mg}Tc nuclear reaction to monitor proton beams: New measurements and consequences on the earlier reported data. Nucl. Instrum. Methods Phys. Res. B 198, 183–196.

Tanaka, S., 1960. Reactions of nickel with alpha-particles. J. Phys. Soc. Japan 15 (12), 2159–2167. http://dx.doi.org/10.1143/JPSJ.15.2159.

Uddin, M.S., Rumman-uz Zaman, M., Hossain, S.M., Qaim, S., 2014. Radiochemical measurement of neutron-spectrum averaged cross sections for the formation of ^{64}Cu and ^{67}Cu via the (n,p) reaction at a TRIGA mark-II reactor: Feasibility of simultaneous production of the theragnostic pair ^{64}Cu/^{67}Cu. Radiochim. Acta 102 (6), 473–480. http://dx.doi.org/10.1515/ract-2013-2199.

Ziegler, J.F., Manoyan, J.M., 2013. The stopping of ions in compounds. Nucl. Instrum. Methods B 35, 215, URL http://www.srim.org.